Unsteady Reverse-Flow Measurements by Split-Film Probes

Kyuro SASAKI and Masaru KIYA*
Mining College, Akita University, Akita 010, Japan.
**Faculty of Engineering, Hokkaido University.*

Split-film probes have been applied to the measurement of turbulence properties in an intermittent reverse-flow region. Two kind of split-film probes of 0.153mm diameter (manufactured by KANOMAX Co. Ltd.) are employed ; one has the split plane normal to the main flow and is able to measure the longitudinal velocity component and reversals of flow direction ; the other has the split plane parallel to the main flow and measures the lateral velocity component. Their response to the magnitude and direction of the velocity vector is statistically calibrated in a uniform flow in a wind tunnel. The frequency response of the probe is checked by comparing the longitudinal velocity spectra with those obtained by a single hot-wire probe in a grid-generated turbulence. The split-film probes are used to measure the reverse-flow region in the separation-reattachment flow formed at the leading edge of a blunt flat plate with square corners. The time-mean, root-mean-square values of the fluctuating velocity and the reverse flow intermittency are successfully obtained by the split-film probes.

1. Introduction

A split-film probe (SFP) has two electrically independent hot films on a single quartz rod [1)-4)]. It is much smaller than a conventional X-array hot-wire probe, so that it can be used to measure velocity fluctuations in a thin layer very close to a wall [1)]. The most important feature of SFP is that it can detect instantaneous reversals of the flow direction.

Two dimensional separated and reattaching flows and nearwakes have recirculating-flow regions near the wall where instantaneous reversals of flow frequently occurs [5)-7)]. In such flow regions most of conventional probes such as hot-wire probes can not be used. At present Laser-Doppler Velocimeters (LDV) are most reliable. The turbulence measurement using an LDV was made by Etheridge and Kemp [6)] in the recirculating zone behind a backward-facing step. Bradbury [5)] measured a highly turbulent flow in the near wake of a normal plate

with a pulsed-wire hot-wire probe. The LDV still requires expensive instrumentation whereas it is difficult to construct small pulsed hot-wire probes.

We feel that SFP is a convenient and simple means to study unsteady reverse flows by conventional constant-temperature anemometer (CTA) circuits, which are now widely used in fluid-dynamics laboratories.

Studies on SFP and its application to flow measurements are reported by several authors. Spencer and Jones[2] obtained a theoretical response function of SFP ; this is used to measure turbulence properties in a boundary layer which is compared with results of conventional hot-wire probes. Blinco and Sandborn[1] showed that SFP can improve the spatial resolution in measuring the structure of wall turbulent shear flows. Hoshino[12] applied SFP to measurements of an axial turbulent jet.

The SFP has not yet been applied to measurements of recirculation zones with intermittent reversals of the flow direction. The purpose of this paper is to present a method of calibrating of SFP, demonstrating its usefulness in unsteady reverse-flow measurements.

2. Experimental apparatus and method

Calibration and measurements were performed in an open-return low-speed air tunnel (Fig. 1) with a 40cm high, 20cm wide and 108cm long working section. The tunnel allows speeds up to 24m/s ; the free-stream turbulence level was 0. 2% at the speed of 20m/s. The velocity distribution in the test section was uniform within $\pm$ 0. 4% exept the turbulent boundary layers on the tunnel walls. The time-mean velocity in the test section was monitored during measurements by the static-pressure difference at the bell entrance of the tunnel.

Two kinds of SFPs (denoted by type A and B) employed in the present study are shown in Fig. 2 . They consist of a 2 mm long active sensor with a diameter of 0. 153mm which have platinum films deposited on a 4 mm long quartz rod. Type A and B are respectively KANOMAX MODEL 1288 and 1287. The type A had the split plane parallel to the axis of the support ; this was used to detect reversals of the longitudinal flow direction and the longitudinal component velocity. On the other hand, the type B had the split-plane perpendicular to the axis of the support and was used to measure the lateral-velocity component.

The SFPs were separately mounted on a mechanism shown in Fig. 3 when they were calibrated. The mechanism consists of a 90°-elbow, a probe support and a cylindrical worm gear. The SFP can be rotated in the plane perpendicular to the axis of the support by means of the worm gear. Accordingly, the angle of incidence of the split plane to the uniform flow can arbitrarily be adjusted within an accuracy of 0. 1°. The whole mechanism was mounted on another traversing mechanism outside the tunnel.

Two semicylindrical hot-film segments of each SFP were heated to an equal constant temperature by two CTAs (KANOMAX SYSTEM 7000). Initial Setting of SFP and CTAs and split-plane alignment were made according to the instruction manuals[3)4)] ; the over-heat ratio of 1.5 was used.

Two CTA outputs were simultaneously recorded on two channels of an analogue tape-recorder (KYOWA R520A ; a cut-off frequency of 10kHz) and later digitized and again recorded on a digital tape-recorder (TEAC DR2000). The magnitude and direction of the velocity vectors were later obtained by a computer (HITAC M200H SYSTEM). This system was originally constructed to obtain a conditional averaging of the velocity fluctuations in large vortex structures in a separation zone. This system can be modified to a real-time system by the use of a personal computer with two A/D converter circuits directly connected to two CTAs respectively.

3. Results and discussion

3. 1 Static calibration

3. 1. 1 Magnitude of velocity vector

In the interest of space, results will be presented only for the type A (see Fig. 2). The cartesian coordinate (x, y) are defined in such a way that the y-axis lies in the split plane, and the x-axis is normal to the y-axis. Figure 4 shows a schematic distribution of local heat-transfer rate $h(\alpha)$ at a SFP surface, where the angle α is measured from the split plane. The magnitude of the velocity vector is denoted by U_N. The profile of $h(\alpha)$ is symmetric with respect to the flow direction θ measured from the x-axis; θ is related to α ($\theta = \alpha - 90^\circ$) .

The heat-transfer rate was calculated from the output of the CTA operating the SFP. If Q_1 and Q_2 respectively denote the rate of heat-transfer from the upstream and downstream films, the difference between Q_1 and Q_2 attains a maximum when the velocity vector is in the x-direction ($\theta = 0^\circ$). The total heat transfer Q^* ($=Q_1+Q_2$) should be a function of U_N alone, being independent of θ. Figure 5 shows the extent to which Q^*/Q^*mean is independent of θ, where Q*mean implies the average value of Q^*. This ratio is seen to be unity within 1.5%. This small deviation in Q^* was probably due to the effet of the two split lines of 13 μm in width.

The total heat transfer rate may be expressed in the following form according to Kings Law[9)]

$$U_N = A(Q_1 + Q_2 - Q_{1n} - Q_{2n})^m, \tag{1}$$

where Q_{1n} and Q_{2n} are the heat transfer rate at $U_N = 0$, m is an exponent and A denotes a constant depending primarily on the property of fluid. An

experiment to determine the exponent m was performed for various values of θ in a range $U_N = 4 \sim 22$m/s.
Using the method of least squares, m was determined as 1.73 ± 0.01 which is independent of θ. This is less than the value of 2.0 for conventional single hot-wires, probably because Reynolds number, *Red*, based on the diameter d and U_N are different from each other[9]. Figure 6 shows the relation of Eq.(1), in which $Q = Q^* - Q_{1n} - Q_{2n}$ and Q_0 is an optional constant of the dimension of heat-transfer rate. Q_0 has been determined so that $(Q/Q_0)^{1.73} = 10$ at $U_N = 20$m/s.

3. 1. 2 Direction of veiocity vector

The difference between Q_1 and Q_2 is a function of the direction of the velocity vector θ (see Fig. 3). Reversals of the flow direction can be determined by comparing Q_1 and Q_2. If Q_1 is less than Q_2, The instantaneous flow is in the direction from the film 2 to the film 1 and vice versa. From a numerical simulation, Apelt[8] shows that the following ratio C is suitable for the detection of the angle θ.

$$C = (Q_1 - Q_2) / Q \tag{2}$$

Figure 7 shows C/Cm as a function of θ, where Cm is a maximum value of C at $\theta = 0°$, This result can be closely approximated by

$$\cos\theta = C/Cm. \tag{3}$$

Equation (3) determines $\cos\theta$ in terms of measured C/Cm. It should be noted, however, that $\sin\theta$ is indeterminate because the type A can not differentiate between θ and $-\theta$.

The type B whose split plane coincides with the x-axis, on the other hand, can determine $\sin\theta$ by the relation $\sin\theta = C/Cm$. To determine $\cos\theta$ or $\sin\theta$, the value of Cm must be given in advance as a function of U_N or Red ($= U_N d/\nu$, ν ; the kinetic viscosity). This is plotted in Fig. 8 which also contains Apelt's numerical result in a range $Red < 40$. The symbol ♦ in Fig. 8 shows that U_N (< 4 m/s) was obtained from Eq.(1). Cm increases sharply with increasing U_N up to $U_N \sim 10$m/s in the same way as the numerical result[8], while for a larger velocity Cm becomes almost unchanged. We assume an empirical relation of the form,

$$\begin{aligned} Cm &= a_0 U_N^{\epsilon} \quad (Red < 100) \\ Cm &= a_1 - a_2 U_N \quad (Red \geqq 100) \end{aligned} \tag{4}$$

where a_0, a_1 and a_2 are constants and ϵ is an exponent. These values can be

determined so as to have the best fit to the measured data. The value of Cm was obtained at each run of the experiment. The exponent was almost constant (0.2), and the correlation coefficient between measured and interporated (by (Eq.(4)) values of Cm was about 0.98.

From the above calibration procedure, the velocity vector can be determined as follows: (i) calculate the magnitude of the velocity vector U_N from Eq.(1); (ii) calculate $cos\theta$ or $sin\theta$ from Eq.(2),(3) and (4); (iii) calculate the velocity components in the x- and y-directions by $U_N cos\theta$ and $U_N sin\theta$; (iv) calculate the time history of two fluctuating velocity by repeating (i)~(iii) at each time.

3. 2 Frequcncy response

To test the frequency response, the SFPs were placed in a grid-generated turbulent flow whose time-mean velocity and turbulence intensity were 13 m/s and 5.8% . The frequency response of the SFPs was checked by comparing the spectra of the longitudinal velocity fluctuation u' with those obtained by a single hot-wire probe. This hot-wire was a tungsten wire of 5 μm diameter with a working length of about 1 mm; square-wave tests showed the maximum frequency of response to be about 10kHz. Let Fourier components of u' measured by the SFP and the single hot- wire probe be respectively denoted by a_s and a_h . Then the ratio $G_f (= a_s/a_h)$ plotted against the frequency becomes as shown in Fig. 9 . This ratio G_f is 1.0 ± 0.1 up to at least 1.5kHz, decreasing gradually in the higher frequency range. This suggests that the velocity fluctuations measured by SFPs are reliable for frequencies less than 1.5kHz, which correspond to wave numbers less than $0.017\ U_\infty/d$ when U_∞ = 13 m/s.

3. 3 An application

The SFPs(type A and B) were tested in a separated-and-reattaching flow (separation bubble) formed along the sides of a blunt flat-plate with square corners [7) 10)] . The configuration of the flow and definition of symbols are illustrated in Fig.10. The cartesian coordinates (x,y) are defined in such a way that the x-axis is in the longitudinal direction and the y-axis vertically outwards from a side. The origin is located at one of the separation edges of the plate whose thickness is denoted by $2H$. The measurements were made at a free-stream velocity U_∞ = 20m/s.

The time-mean reattachment length x_R was $10.1H$ [11)] at this velocity.

Figure 11 (a) and (b) shows measured profiles of the longitudinal time-mean velocity U and the r.m.s. velocity $\overline{(u'^2)}^{\frac{1}{2}}$ in a crossflow section x/H = 6 , together with those obtained by the single hot-wire probe[7)10)]. The time-mean output of the hot-wire probe was interpreted as the reverse-flow velocity in a region where the reverse flow intermittency Ir is greater than 0.5. The results of the SFP and the

hot-wire agree fairly well in regions where $Ir \gtrsim 0.9$ and $Ir \lesssim 0.1$. However, the nearer the Ir is to 0.5, the greater the difference between the two results. This is mainly because the single hot-wire can not detect the reversals of the flow direction and because it it becomes unreliable when the yaw angle fluctuation is not sufficiently small.

Figure 12 shows a probability density Pd of the longitudinal velocity $u(=U+u')$ obtained at a position ($x/H=6$, $y/H=0.8$) where U is approximately zero. The well-documented pulsed-wire probes[5] fail to give signals when $U \sim 0$ and this yields a significant dip of the probability density function $Pd(u)$ near $U=0$.

As shown in Fig.12, no missing of $Pd(u)$ occurs near $U=0$ for the SFP. This result strongly suggests that the SFP can detect zeros of the longitudinal velocity, i.e. $U_N \cos\theta = 0$ exept when $U_N = 0$.

Thus we feel that the SFP is superior to a pulsed-wire probe.

Figure 13 shows the reverse-flow intermittency Ir as a function of $U/(\overline{u'^2})^{\frac{1}{2}}$. The solid line in the figure is given

$$Ir=\frac{1}{2}\left\{1-erf\left[\frac{U}{(\overline{u'^2})^{\frac{1}{2}}}\right]\right\} \tag{5}$$

where erf is the error function. This equation has been obtained on the assumption that the probability density of u' is Gaussian in intermittently reverse flow regions [10) 13)](see Fig.12).The measured Ir is seen to be well represented by Eq.(5). It is possible that the relation (5) is generally true for two-dimensional reverse-flow regions of similar configurations. This relation can perhaps be used to find the suitability of a probe to be developed for the measurement of reverse flow regions.

Figure 5 and 6 compare the lateral r.m.s. velocity $(\overline{v'^2})^{\frac{1}{2}}/U_\infty$ and Reynolds shear stress $-\overline{u'v'}/U^2_\infty$ measured by the SFP of type B with those obtained by an X-array hot-wire probe. It should be noted that $-\overline{u'v'}$ measured by SFP is reliable only in regions where no instantanious reverse flow occurs. The maximum values of $(\overline{v'^2})^{\frac{1}{2}}$ and $-\overline{u'r'}$ obtained by the SFP is respectively by about 20 % and 30 % larger than the hot-wire results. This is reasonable because the SFPs can detect the fluctuating components u' and v' even when the direction of local flow changes considerably if no flow reversals exist.

4. Conclusion

The split-film probes have been shown to be reliable and economical tool for tubulence measdrements in the intermittent reverse-flow regions.

A method of calibration of the magnitude and direction of the velocity vector is presented. An exponent and a few constants included in the calibration formulae are obtained and used to successfully measure the time-mean velocity, unsteadiness and turbulence properties in a leading-edge separation bubble.The frequency

response is tested in a grid-generated turbulence in terms of the power spectra of the longitudinal velocity fluctuations. This test has shown that the SFPs can detect the velocity fluctuations less than about 1.5kHz at a time-mean velocity of 13 m/s. The probability density of the longitudinal velocity fluctuation shows no dip near zero time-mean velocity, which is usually observed in that obtained by pulsed hot-wire probes.

It is expected that if a cylindrical hot-film is divided into four equivalent segments, the instantaneous velocity vector can be measured even in intermittently reverse flow regions.

Referrences

1) Blinco,P.H. and Sandborn,V.A.: Use of the Split-Film Sensor to Measure Turbulence in Water near a Wall, Proc. Symp. Turbulence in Liquids (1975), 403.

2) Spencer,B.W. and Jones,B.G.: Turbulence Measurements with the Split-Film Anemometer Probe, Proc. Symp. Turbulence in Liquids (1971),7.

3) Thermo-System Inc.: TSI Split-Film Sensor Calibration and Applications, Tech. Bull. TB-20.

4) Kuranobu,T.: Calibration and Application of Split-Film Sensor, KANOMAX Corp. Tech. Bull. HWA-**32**,(1979)[in Japanese].

5) Bradbury,L.J.S.: Measurements with Pulsed-Wire and Hot-Wire Anemometer in Highly Turbulent Wake, J. Fluid Mech.,**77**(1976), 437.

6) Etheridge,D.W. and Kemp,P.H.: Measurements of Turbulent Flow Downstream of a Rearward-Facing Step, J. Fluid Mech.,**86**(1978), 545.

7) Sasaki,K. and Kiya,M.: Structure of a Turbulent Separstion Bubble(2 nd Report, Measurements by a Conditional Sampling Technique), Trans. JSME,B**49**-447(1983),2610 [in Japanese].

8) Apelt,C.J.: Characreristics of Split Film Sensor, AIAA J., **17**-1(1979),101.

9) Collins,D.C. and Williams,M.T.: Tow-Dimensional Convection from Heated Wires at Low Reynolds Numbers, J. Fluid Mech., **6** (1959),357.

10) Sasaki,K. and Kiya, M.: Unsteady Reverse-Flow Characteristics and a Possible Mechanism of High Heat-Transfer Rate in a Turbulent Separation Bubble, Trans. JSME,B**50**-458(1984),2549 [in Japanese].

11) Kiya,M. and Sasaki,K.: Structure of a Turbulent Separation Bubble, J. Fluid Mech.,137(1983),83.

12) Hoshino,E.: Measurements with Split-Film Sensor in a Turbulent Jet, Preprint of JSME,No.921(1983), 3 [in Japanese].

13) Kiya, M. and Sasaki, K.: Turbulence Structure and Unsteadiness in a Separation-Reattachment Flow, 5 th Turbulent Shear Flows Symp. (1985), 5 . 7 .

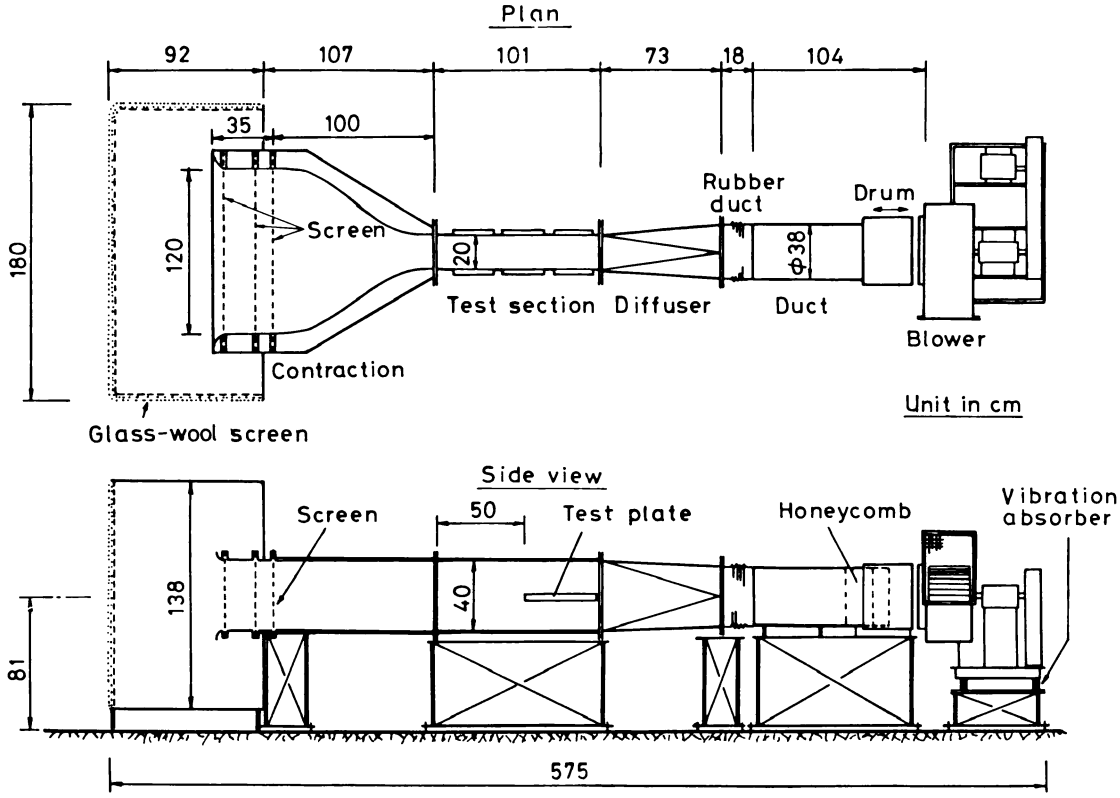

Fig. 1 Wind tunnel

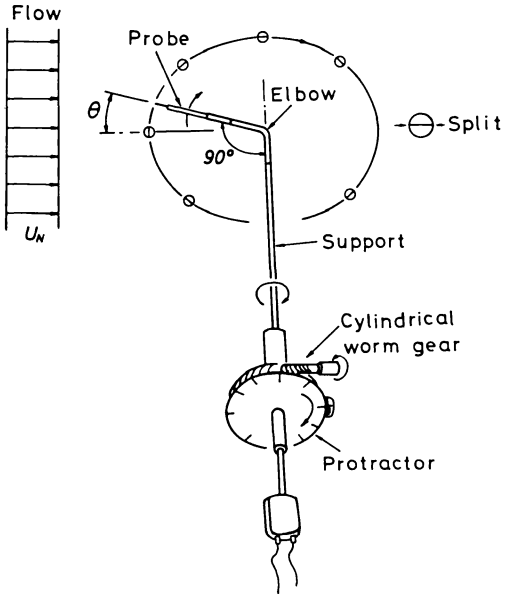

Fig. 3 Supporting mechanism to chsnge yaw angle of split-film probe.

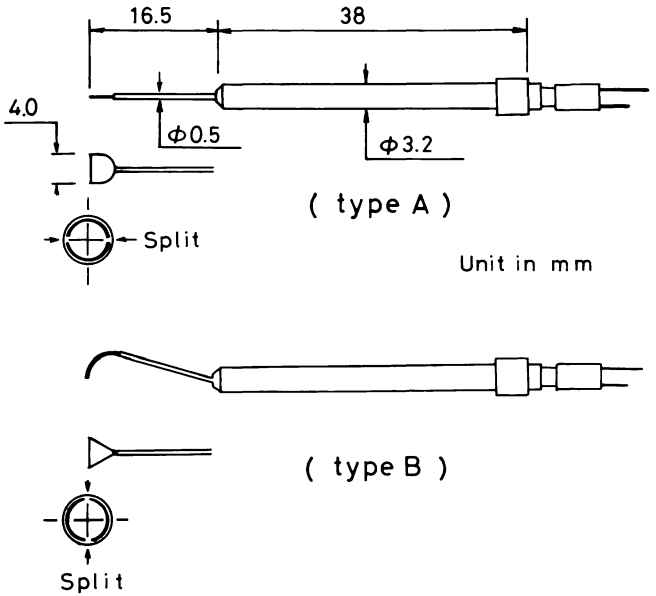

Fig. 2 Split-film probes. Type A and B are respectively KANOMAX model 1288 and 1287.

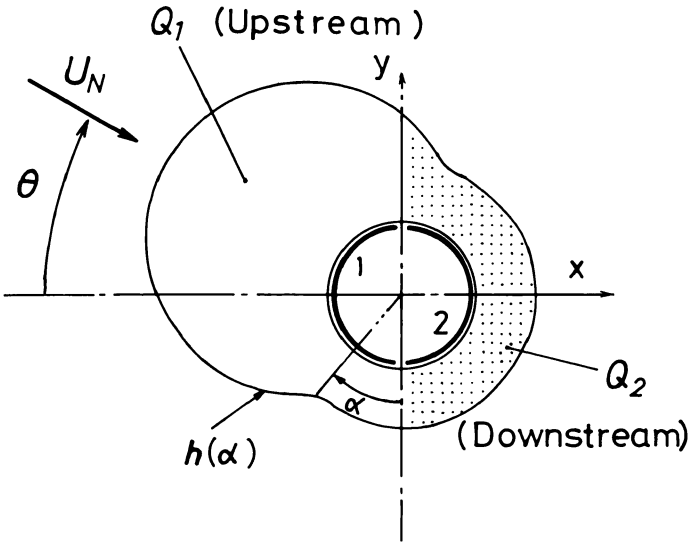

Fig. 4 Schematic distribution of local heat-transfer rate $h(\alpha)$ at the surface of a split-film probe.

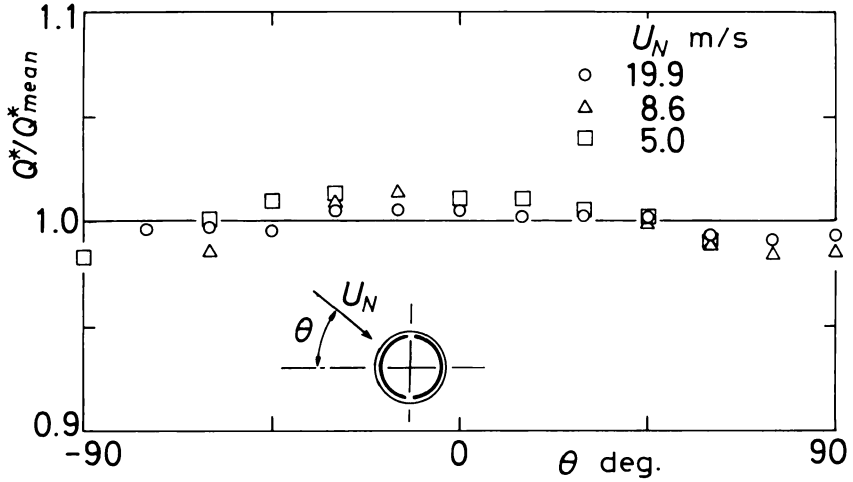

Fig. 5 Dependence of total heat-transfer rate Q^* on direction of velocity vector θ.

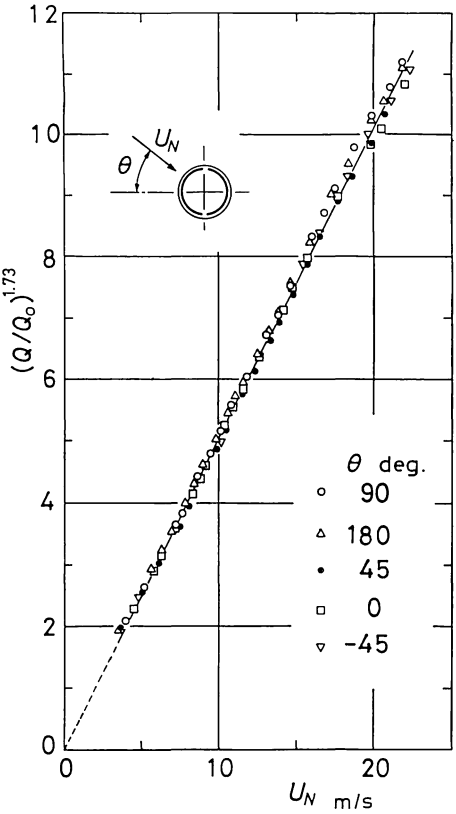

Fig. 6 Heat transfer rate Q plotted against magnitude of velocity vector U_N: Q_0 is a constant so chosen that $(Q/Q_0)^{1.73}=10$ at $U_N = 20$ m/s.

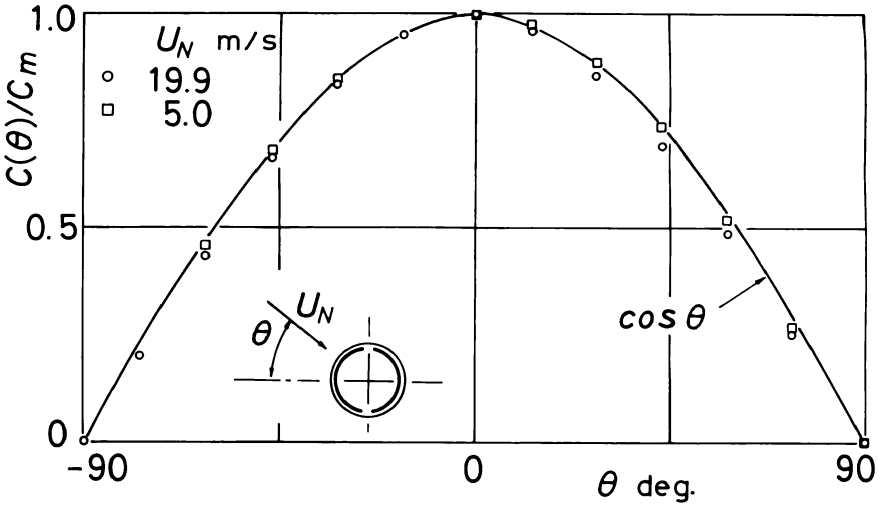

Fig. 7 Distribution of C [$= (Q_1 - Q_2)/Q$] as a function of direction of velocity vector θ.

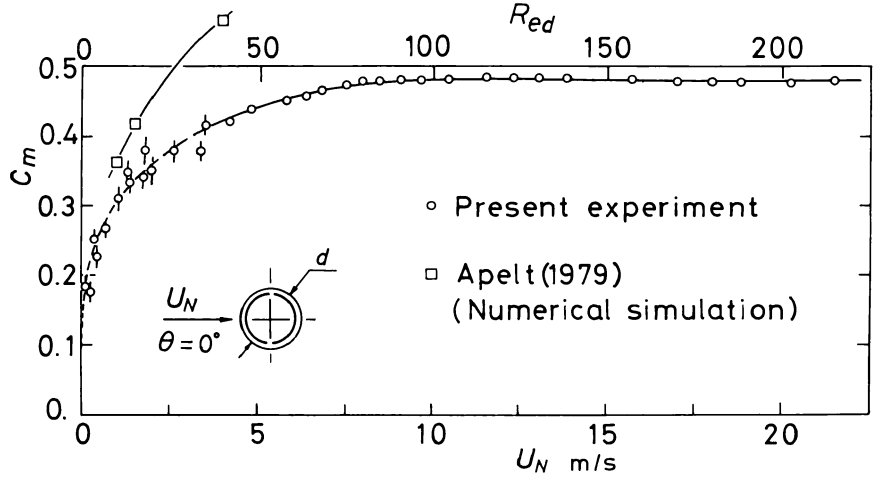

Fig. 8 Value of Cm as a function of U_N and Reynolds number Re_d based on diameter d of a split-film probe.

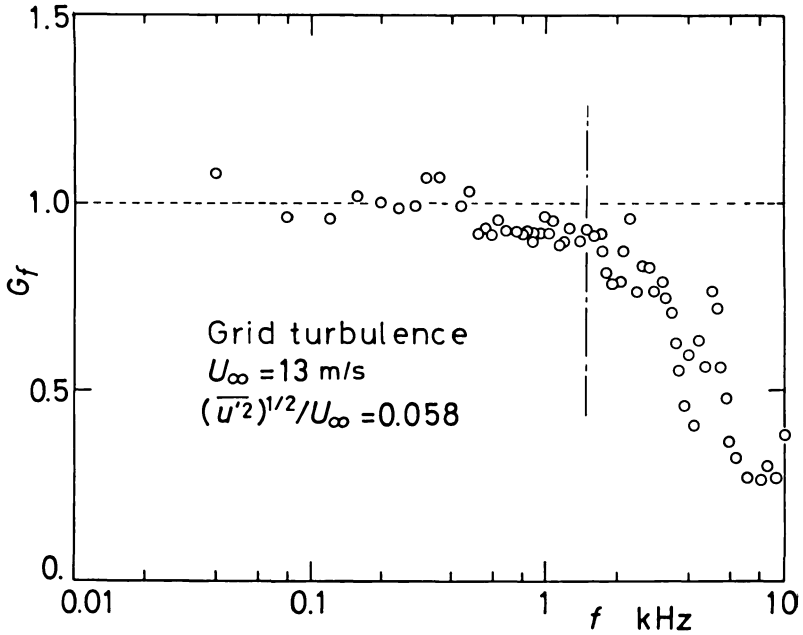

Fig. 9 Frequency response of a split film probe.

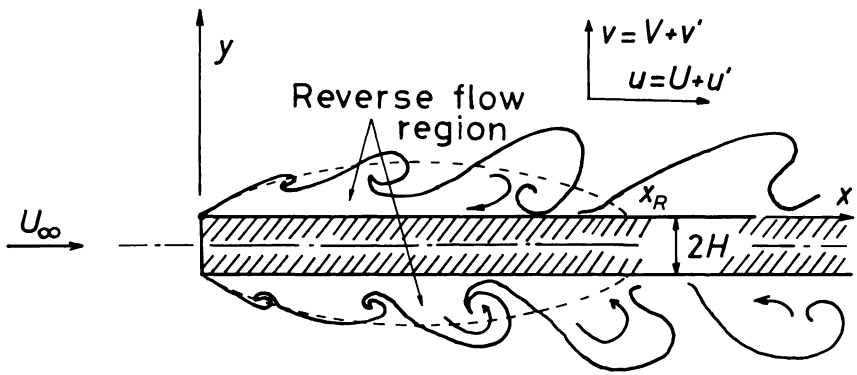

Fig.10 Configuration of separated-and-reattaching flow in which split-film probe are tested. Broken lines denote boundaries of time-mean recirculating zones.

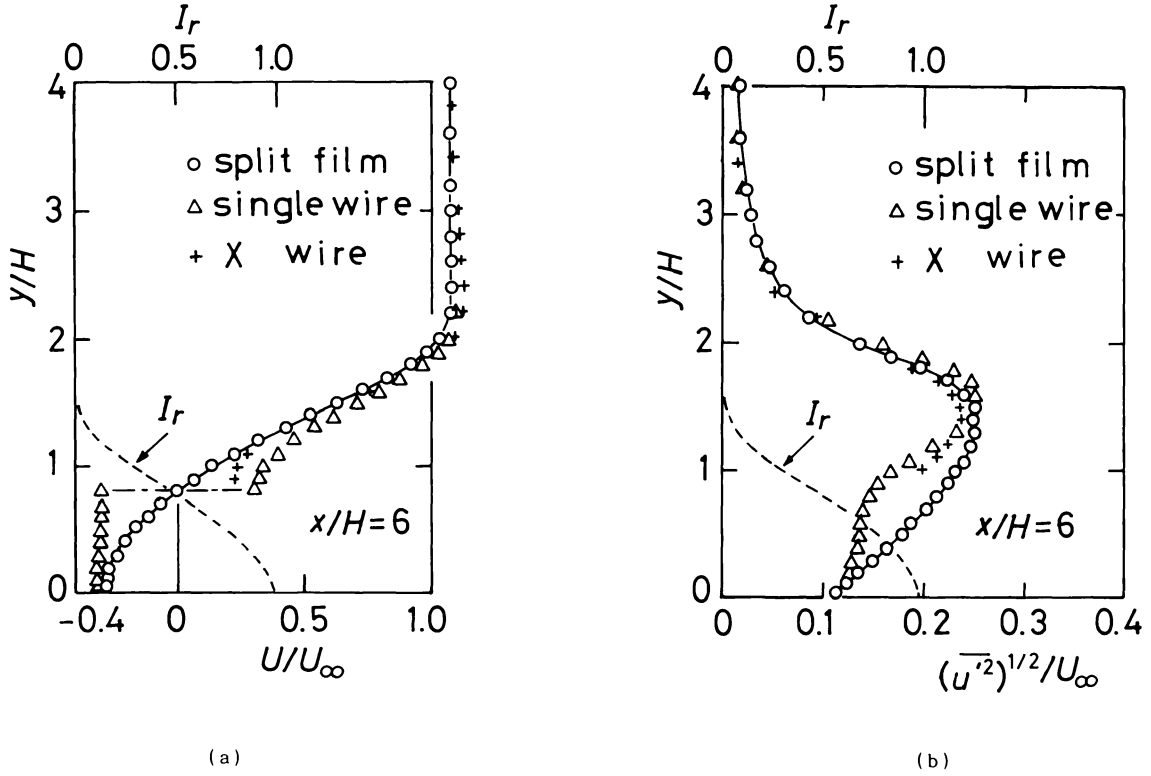

Fig.11 Distributions of (a) time-mean longitudinal velocity U and (b) root-mean square values of longitudinal velocity fluctuation $(\overline{u'^2})^{\frac{1}{2}}$.

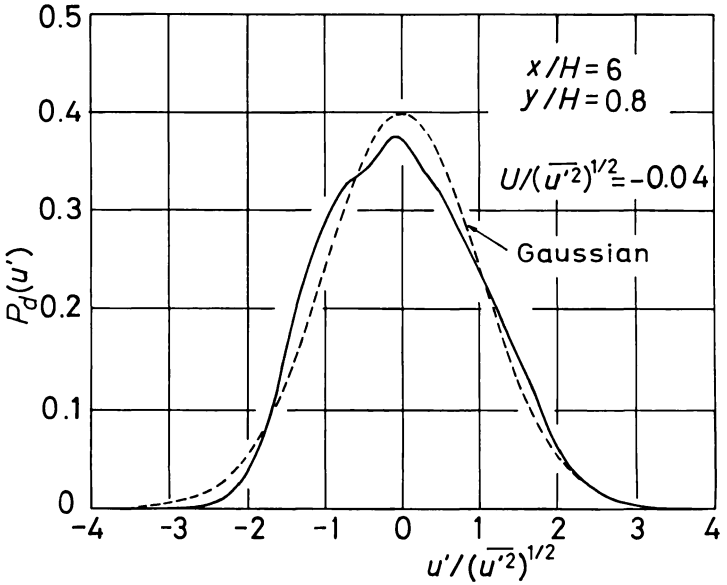

Fig.12 Probability density Pd of longitudinal velocity $u(=U+u')$ at position of $U \sim O$.

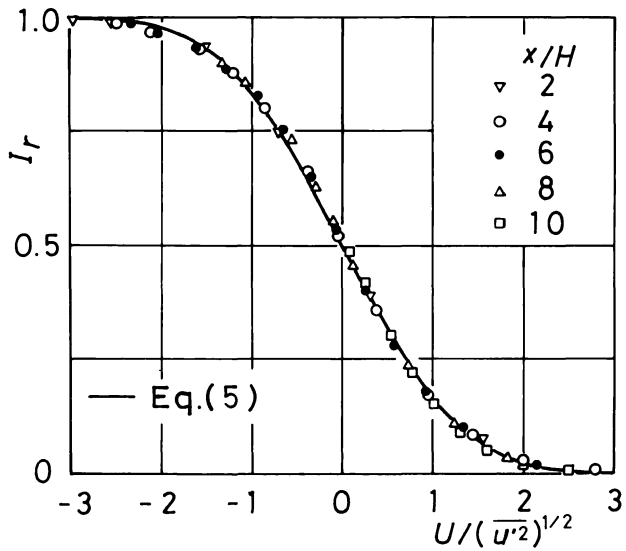

Fig.13 Reverse-flow intermittency Ir as a function of $U/(\overline{u'^2})^{\frac{1}{2}}$.

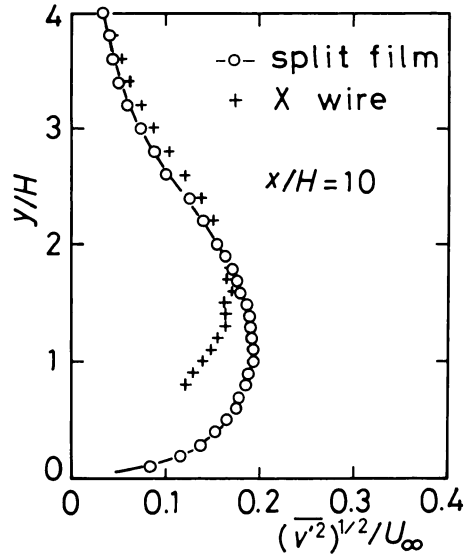

Fig.14 Distribution of root-mean square value of lateral velocity fluctuation $(\overline{v'^2})^{\frac{1}{2}}$ above reattachment line x/H=10.

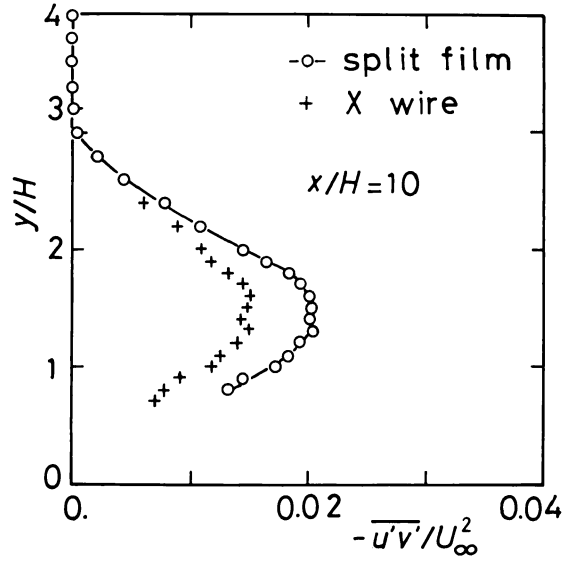

Fig.15 Distribution of Reynolds shear stress $-\overline{u'v'}$ above reattachment line x/H =10.